PROCEEDINGS OF SPIE

Thermoelectric bolometers based on silicon membranes

Aapo Varpula, Andrey V. Timofeev, Andrey Shchepetov, Kestutis Grigoras, Jouni Ahopelto, et al.

SPIE.

Thermoelectric bolometers based on silicon membranes

Aapo Varpula*, Andrey V. Timofeev, Andrey Shchepetov, Kestutis Grigoras, Jouni Ahopelto, and Mika Prunnila

VTT Technical Research Centre of Finland Ltd, Espoo, P.O. Box 02044, Finland

ABSTRACT

State-of-the-art high performance IR sensing and imaging systems utilize highly expensive photodetector technology, which requires exotic and toxic materials and cooling. Cost-effective alternatives, uncooled bolometer detectors, are widely used in commercial long-wave IR (LWIR) systems. Compared to the cooled detectors they are much slower and have approximately an order of magnitude lower detectivity in the LWIR. We present uncooled bolometer technology which is foreseen to be capable of narrowing the gap between the cooled and uncooled technologies. The proposed technology is based on ultra-thin silicon membranes, the thermal conductivity and electrical properties of which can be controlled by membrane thickness and doping, respectively. The thermal signal is transduced into electric voltage using thermocouple consisting of highly-doped n and p type Si beams. Reducing the thickness of the Si membrane improves the performance (i.e. sensitivity and speed) as thermal conductivity and thermal mass of Si membrane decreases with decreasing thickness. Based on experimental data we estimate the performance of these uncooled thermoelectric bolometers.

Keywords: long-wave infrared, thermal detector, bolometer, thermoelectric, thermocouple, silicon, membrane

1. INTRODUCTION

State-of-the-art high performance IR sensing and imaging systems utilize highly expensive photodetector technology, which requires cooling and exotic materials that are often toxic (e.g. HgCdTe). These limit their use mainly to scientific and military applications. Cost-effective alternatives, uncooled bolometer detectors, are widely used in commercial long-wavelength IR (LWIR) systems. Compared to the cooled detectors they are much slower and have approximately an order of magnitude lower detectivity in the LWIR.

In this work, we discuss an uncooled bolometer technology, which is foreseen to be capable of narrowing the gap between the cooled and uncooled technologies. We have demonstrated this technology experimentally very recently[1]. It is based on ultra-thin highly-doped silicon membranes[1,2]. The high sensitivity of this technology arises from low phonon thermal conductivity of the ultra-thin silicon membrane[3,4]. The high speed is provided by the extremely small thermal mass of the ultra-thin silicon membrane. In this work, we estimate the performance of these thermal detectors when they are equipped with thin film absorbers.

2. BOLOMETER FUNDAMENTALS

A bolometer is a device that measures the power of incident thermal radiation. The word originates from Greek word 'bolē' meaning beam of light. Often, mainly due to the historical reasons the definition of bolometer is limited to a specific type of bolometer, the resistive bolometer invented by S. P. Langley. Here we adopt a wider definition to cover other similar types of thermal detectors as well.

A schematic of a bolometer is shown in Figure 1. Incident thermal radiation is absorbed in the absorber of the bolometer, which is thermally isolated from the ambient and the substrate on which the bolometer is fabricated. Often vacuum is used as an efficient thermal isolation. The absorber supporting beams hold the absorber above the substrate and connect the bolometer to the readout electronics, but they also form an unavoidable thermal link to the bolometer supports. The

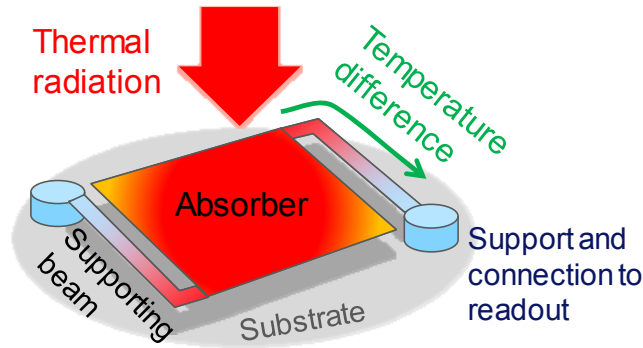*aapo.varpula@vtt.fi; www.vttresearch.com / www.vtt.fi

Figure 1. A schematic picture of a bolometer: Absorber absorbs the incident thermal radiation, and supporting beams connect the absorber to readout electronics. A transducer located either within the absorber or on/in the supporting beams transduces the thermal signal into electric signal.

absorption of thermal radiation increases the temperature of the absorber, which is detected with a transducer, which transduces the thermal signal into electrical signal. In the case of resistive bolometers this transducer is a resistor which changes its resistance when temperature is changed[5,6]. An external voltage or current needs to be supplied in order to measure this resistance change. In a thermoelectric bolometer the transducer is a thermocouple or thermopile[5], where the Seebeck effect generates the output voltage due to a thermal gradient along the bolometer supporting beams, which in this case work simultaneously as thermocouple or thermopile legs. The thermocouple or thermopile is made of two different materials with dissimilar Seebeck coefficients. Metals and semiconductors can be used as well as a semiconductor with n-type and p-type doping.

Here we have listed the main functional parts of the bolometer. In real bolometers the number of subparts can be smaller if each subpart has several functions. In addition, real bolometers can have additional mechanical supporting structures and electrical insulating layers. Furthermore, optics and optical subcomponents such as back reflectors often used in bolometers are discussed for example in Ref. 7.

3. MODEL OF THERMOELECTRIC BOLOMETER

3.1 General bolometer model

A bolometer is a device whose absorber is heated up with incident thermal radiation. The corresponding heater power is given by ηP, where P is the incident optical power on the total detector area, and the total optical efficiency is given by

$$\eta = \eta_{\text{abs}}\eta_{\text{FF}}, \tag{1}$$

where η_{abs} is the combined optical efficiency of the absorber and the optics, and the fill factor (FF) is given by

$$\eta_{\text{FF}} = \frac{A_{\text{abs}}}{A}, \tag{2}$$

where A is the total area occupied by the detector and A_{abs} is the area of the absorber. In the absence of self-heating effects potentially present in resistive bolometers, the heat balance is given by

$$\eta P = G_{\text{th}}\Delta T + C_{\text{th}}\frac{d\Delta T}{dt}, \tag{3}$$

where G_{th} is the total thermal conductance of all thermal links connecting the absorber to the substrate and the ambient, C_{th} is the heat capacity of the device, and ΔT is the temperature difference between the absorber the substrate. Solving eq. (1) in frequency domain gives the responsivity of the bolometer as (cf. Refs. 1, 5 and 6)

$$\frac{dV}{dP} = \frac{dV}{dT} \cdot \frac{\eta}{G_{\text{th}}\sqrt{1+\tau^2\omega^2}}, \tag{4}$$

where ω is the angular frequency, and the thermal time constant is given by

$$\tau = \frac{C_{\text{th}}}{G_{\text{th}}}. \tag{5}$$

Equation (4) shows that the bolometer should be operated at low frequencies, well below the thermal cut-off described by τ, for maximal responsivity. In this range equation (5) reduces to

$$\frac{dV}{dP}(\omega = 0) = \frac{dV}{dT} \cdot \frac{\eta}{G_{\text{th}}}. \tag{6}$$

In addition to the speed of the bolometer described by τ, the common figures of merit of bolometers are noise equivalent power (NEP) and specific detectivity D^*. Noise equivalent power (NEP) equals to the input power that produces an output signal with signal-to-noise ratio (SNR) of unity, SNR = 1, at specific bandwidth[5,6]. In this work, all the values are reported in respect to the unit frequency bandwidth.

In bolometers the main sources of noise[1,5,6] are the phonon noise originating from thermal fluctuations and the Johnson-Nyquist noise of the electrical resistance of the thermoelectrical transducer, which is a temperature-sensitive resistor in the case of resistive bolometer, and a thermocouple in the case of thermoelectric bolometers. In the optimal frequency range well below the thermal cut-off, the corresponding NEPs of the phonon and Johnson-Nyquist noises are given by

$$NEP_{\text{ph}} = \frac{1}{\eta}\sqrt{4k_{\text{B}}T^2 G_{\text{th}}}, \tag{7}$$

and

$$NEP_{\text{JN}} = \frac{\sqrt{4k_{\text{B}}TR}}{\frac{dV}{dP}(\omega=0)} = \left(\frac{dV}{dT}\right)^{-1} \cdot \frac{G_{\text{th}}}{\eta}\sqrt{4k_{\text{B}}TR}, \tag{8}$$

respectively. Here k_{B} is the Boltzmann constant, T is the absolute temperature (in this work $T = 300$ K), and R is the total resistance of the thermoelectrical transducer. The total NEP of these uncorrelated noise sources is given by

$$NEP = \sqrt{NEP_{\text{JN}}^2 + NEP_{\text{ph}}^2}. \tag{9}$$

Here we focus on these main sources of noise and neglect the other additional noise sources[5,6,8] such as 1/f and amplifier noise. In the ideal case, 1/f noise is not present in thermoelectric bolometers. The specific detectivity is given by[5,6]

$$D^* = \frac{\sqrt{A}}{NEP}. \tag{10}$$

3.2 Model of thermoelectric bolometers based on membranes

Here the general model presented above is applied to thermoelectric bolometers, were the temperature difference between the absorber and the substrate is converted into electric signal using the thermocouple, the total Seebeck coefficient of which, is given by

$$\frac{dV}{dT} = S = S_{\text{p}} - S_{\text{n}}, \tag{11}$$

where S_{p} are S_{n} the Seebeck coefficient of the p-type and n-type materials, respectively.

The thermoelectric legs, i.e. supporting beams, of the bolometer are fabricated from membrane with thickness of t. The length and width of the n-type leg is l_{n} and w_{n}, respectively, whereas for the p-type leg they are l_{p} and w_{p}, respectively. In the case of membrane-based devices it is convenient to describe device geometries using number of squares. The number of squares in the n-type leg is given by

$$N_{\square\text{n}} = \frac{l_{\text{n}}}{w_{\text{n}}}, \tag{12}$$

The number of squares in the p-type leg is given by

$$N_{\square\text{p}} = \frac{l_{\text{p}}}{w_{\text{p}}}, \tag{13}$$

The total electric resistance of the thermocouple is given by

$$R = R_{\text{n}} + R_{\text{p}}, \tag{14}$$

where R_n and R_p are the resistances of the n-type and p-type legs, respectively. They are given by

$$R_n = N_{\square n}\frac{\rho_n}{t},\qquad(15)$$

and

$$R_p = N_{\square p}\frac{\rho_p}{t},\qquad(16)$$

where ρ_n and ρ_p are the electric resistivities of the n-type and p-type materials, respectively.

The total thermal conductance of the thermocouple is given by

$$G_{th} = G_{th,n} + G_{th,p},\qquad(17)$$

where $G_{th,n}$ and $G_{th,p}$ are the thermal conductances of the n-type and p-type legs, respectively. They are given by

$$G_{th,n} = \frac{G_{\square th,n}}{N_{\square n}},\qquad(18)$$

and

$$G_{th,p} = \frac{G_{\square th,p}}{N_{\square p}},\qquad(19)$$

where the sheet thermal conductances of the n-type and p-type materials are, in turn, given by

$$G_{\square th,n} = \kappa_n t,\qquad(20)$$

and

$$G_{\square th,p} = \kappa_p t,\qquad(21)$$

where κ_n and κ_p are the thermal conductivities of the n-type and p-type materials, respectively.

In order to optimize the performance of any thermoelectric device, the effective thermoelectric figure of merit ZT of the device needs to be maximized. This achieved when the ratio n and p-type geometries is optimal[9]. However, for simplicity we assume that $\rho_n \approx \rho_p$ and $\kappa_n \approx \kappa_p$ (i.e. $G_{\square th,n} \approx G_{\square th,p}$), so that the optimal ZT is reached when $N_{\square n} = N_{\square p}$. In the case of silicon the former assumption can be reached by doping, and the latter assumption is rather accurately valid when doping densities of the n and p-type material is equal[10].

In the case of thermoelectric bolometers, NEP can be expressed in a rather compact form. In the optimal frequency range well below the thermal cut-off, NEP can be written using equations (7)-(9) and (11) as[1]

$$NEP = NEP_{ph}\sqrt{1 + \frac{1}{\widetilde{ZT}}} = \frac{1}{\eta}\sqrt{4k_B T^2 G_{th}}\sqrt{1 + \frac{1}{\widetilde{ZT}}},\qquad(22)$$

where $\widetilde{ZT} = S^2 T/(G_{th}R)$ is the effective thermoelectric figure of merit of the thermoelectric bolometer.

In this work it is assumed that heat capacity of the thermoelectric bolometer is given by the absorber only. Here the absorber consists of the thermoelectric membrane and the absorbing layer. The small contribution from the legs is neglected. The heat capacity of the bolometer is given by

$$C_{th} = A_{abs}\big(c_V t + c_{V,abs}t_{abs}\big) = \eta_{FF}A\big(c_V t + c_{V,abs}t_{abs}\big),\qquad(23)$$

where c_V is the volumetric heat capacity of the membrane, $c_{V,abs}$ is the volumetric heat capacity of the absorber material, and t_{abs} is the thickness of the absorber material.

4. RESULTS AND DISCUSSION

The present bolometer model employed in the calculations consists of equations (1), (2), (5)-(21), and (23). The parameter used in this work and their values are listed in Table 1. Seebeck coefficient is taken from Ref. 1 where a 40 nm thick Si membrane bolometer has been demonstrated. Here, we assume that the active material in the absorber is 10 nm of Ti optimized for wavelength of 10 μm[7]. The geometrical parameters used are listed in Table 2. The selected geometrical values represent general features of scaling, but are not representing limitations of specific fabrication process and were not optimized for specific application. Figure 2 shows the experimental thermal conductivity and the sheet thermal conductivity of the ultra-thin silicon membrane which was used as the active part of the thermoelectric bolometer. The phenomenological model fitted to the experimental data shown in Figure 2 was used in all the calculations of this work.

Table 1. Parameters used in the calculations.

Parameter	Value	Material
Thermocouple		
Total Seebeck coefficient S	0.4 mV/K[1]	Heavily doped n and p silicon
n-type resistivity ρ_n	1 mΩcm	Heavily doped n-type silicon
p-type resistivity ρ_p	1 mΩcm	Heavily doped p-type silicon
Absorber		
Combined optical efficiency of absorber and optics η_{abs}	1	
Thickness of absorber t_{abs}	10 nm[7]	Titanium
Volumetric heat capacity of membrane c_V	1.64 MJ/K/m^3	Silicon
Volumetric heat capacity of absorber $c_{V,abs}$	2.63 MJ/K/m^3	Titanium

Table 2. Geometrical parameters used in the calculations.

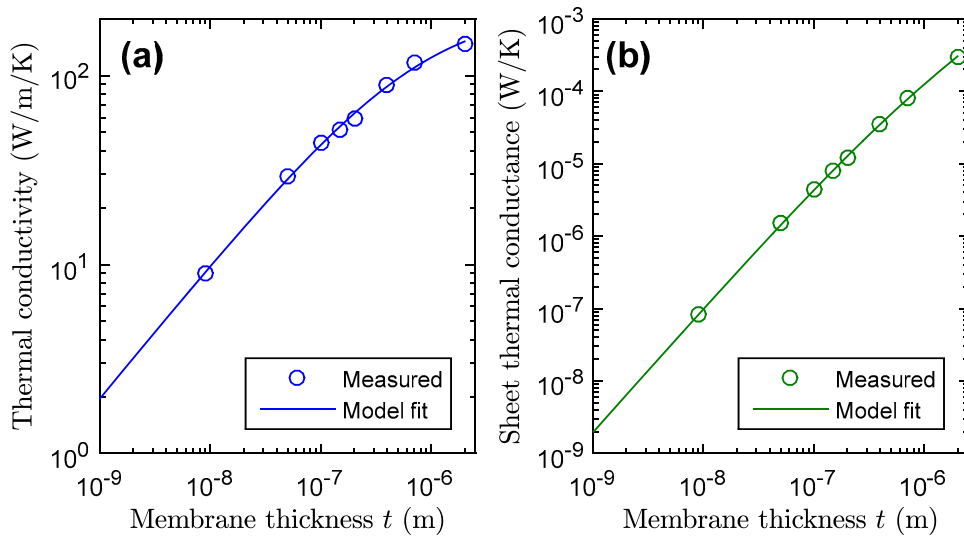| Detector total area A	Fill factor (FF) η_{FF}	Number of squares $N_{\square n} = N_{\square p}$
20x20 μm^2	0.85	20
50x50 μm^2	0.90	50
100x100 μm^2	0.95	100

Figure 2. Experimental data[4] from ultra-thin silicon membranes as functions of membrane thickness: (a) thermal conductivity κ and (b) sheet thermal conductance $G_{\square th} = \kappa t$. A phenomenological model, $\kappa = \alpha/(1 + \beta t^{-\gamma})$, is fitted to the experimental data of (a). The values of the fitting parameters are $\alpha = 228.4$ W/m/K, $\beta = 116.0$ /nm, and $\gamma = 0.7149$.

The calculated characteristics of the proposed thermoelectric bolometers are shown in Figures 3-5. These figures show that both thermal time constant τ and sensitivity of the device increase rapidly when the thickness of the silicon membrane is decreased. The sensitivity increases with decreasing membrane thickness due to decreasing thermal conductance G_{th} caused by decreasing sheet thermal conductance of the thermocouple legs (see Figure 2b and equations (17)-(19) and (7)-(9) or (22)). When the thickness of the Si membrane is 10 nm or below the NEP of all devices is below 1 pW/Hz$^{1/2}$. The dependence of the speed of the devices described by τ is more complex since τ depends on G_{th} as $\tau = C_{th}/G_{th}$ (equation (5)). The heat capacity C_{th} depends linearly (equation (23)) on the membrane thickness and decreases with decreasing membrane thickness. Because increases G_{th} with decreasing membrane thickness more rapidly than C_{th} increases, the combined effect is that τ increases with decreasing membrane thickness.

Figures 4 and 5 shows that the larger the pixel, the larger D^* (due to higher amount of signal gathered), and the larger τ (due to larger thermal mass). Figure 4 shows the specific detectivity D^*, which is limited fundamentally by the background radiation[5,8]. This limit increases when the detector or background temperature decreases. Figure 4 shows that the largest devices have D^* higher than the background radiation limit. This suggests that the signal-to-noise ratio of the largest detectors is not limited by the internal noise sources of the detector. However, it should be noted that in the calculation of the background radiation limit a half sphere radiating into the detector with a full black-body radiation spectrum is considered and, therefore, in real devices with narrow absorption band and field of view the actual limit could be higher.
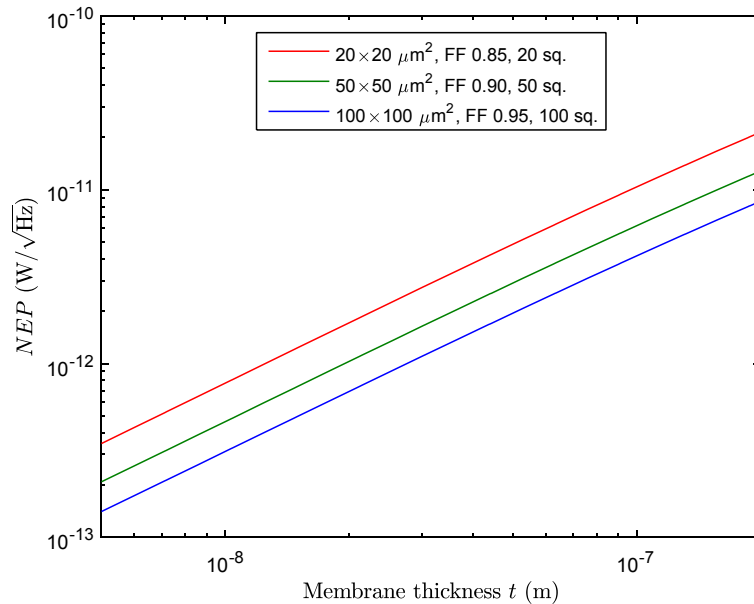
Figure 3. Calculated NEP of the thermoelectric bolometers as functions of the silicon membrane thickness. The parameter values listed in Tables 1 and 2 and the thermal conductivity model of Figure 2 were used in the calculations.
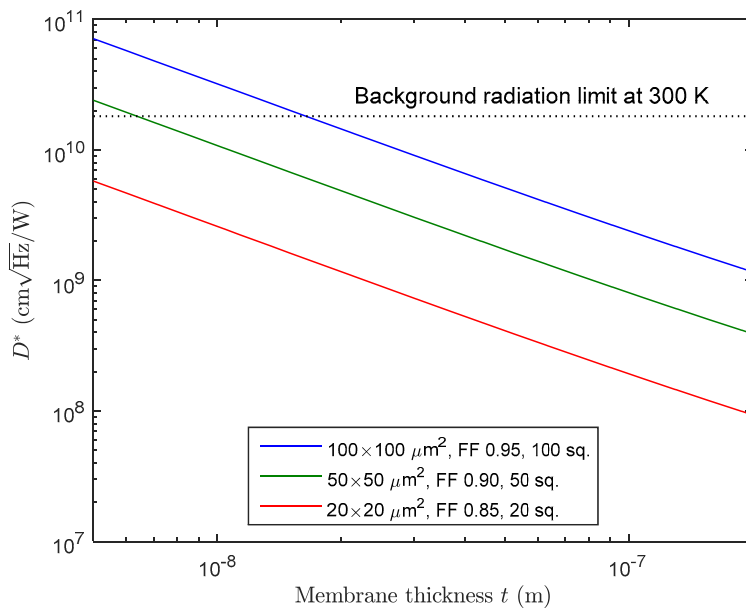

Figure 4. Calculated specific detectivity D^* of the thermoelectric bolometers as functions of the silicon membrane thickness. The parameter values listed in Tables 1 and 2 and the thermal conductivity model of Figure 2 were used in the calculations. The dotted lines shows the fundamental limit for thermal detectors when the detector and background temperature is 300 K.
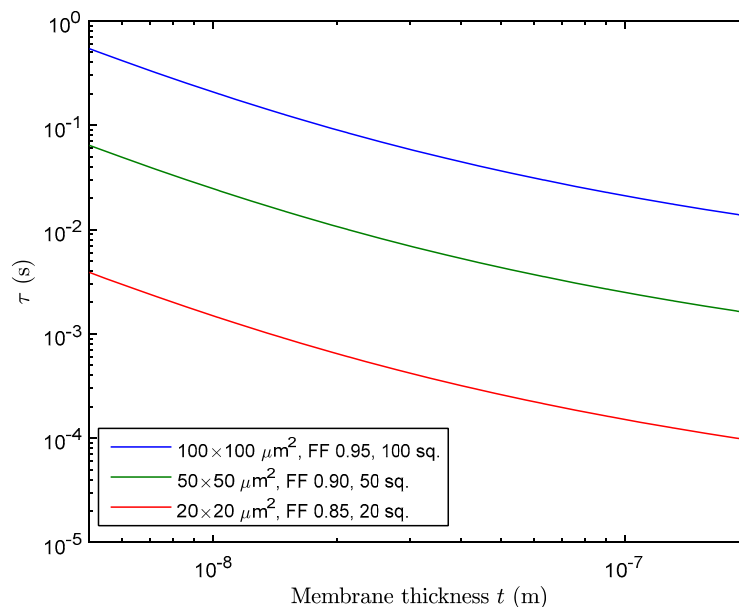
Figure 5. Calculated thermal time constant τ of the thermoelectric bolometers as functions of the silicon membrane thickness. The parameter values listed in Tables 1 and 2 and the thermal conductivity model of Figure 2 were used in the calculations.

In these devices NEP does not depend on the detector area, but in the calculations of Figures 3-5 we have chosen the larger devices to have larger number of squares in the thermocouple legs $N_{\square n}$ and $N_{\square p}$. Changing the number of squares in the legs allows optimization of sensitivity given by NEP and D^* and speed given by τ. The sensitivity increases with increasing number of squares and the speed increases with decreasing number of squares.

To illustrate this effect we have calculated the performance characteristics of the thermoelectric bolometers based on silicon membrane with thickness of 9 nm, with various number of squares in the thermocouple legs. The results are shown in Figures 6-8. As noted above and shown in Figure 6, NEP is the same although the detector areas are different. Figure 7 shows that the smallest detector can have D^* over 10^{10} cmHz$^{1/2}$/W if the thermocouple legs can be designed to have over 100 squares. Figure 8 shows that the largest device can have thermal time constant below 50 ms if it has less than 20 squares in the thermocouple legs.
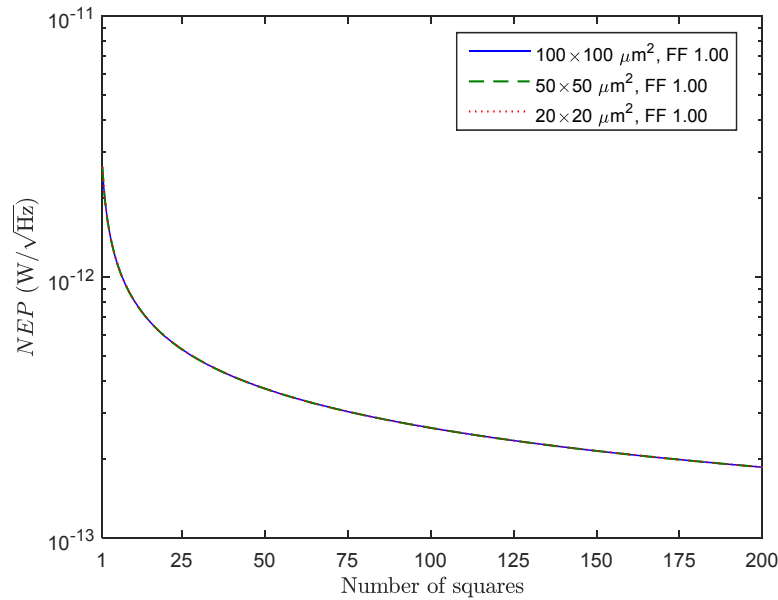
Figure 6. Calculated NEP of the thermoelectric bolometers as functions of the number of squares in the thermocouple legs $N_{\square n} = N_{\square p}$. The indicated detector areas, the parameter values listed in Table 1, $\eta_{FF} = 1$, and the Si membrane thermal conductivity of 9 W/m/K (corresponding to thickness of 9 nm) were used in the calculations.
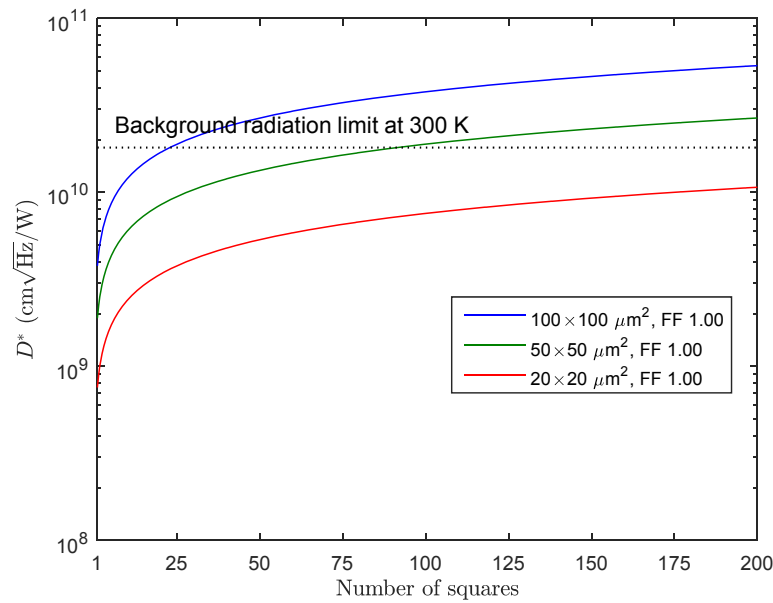

Figure 7. Calculated specific detectivity D^* of the thermoelectric bolometers as functions of the number of squares in the thermocouple legs $N_{\square n} = N_{\square p}$. The indicated detector areas, the parameter values listed in Table 1, $\eta_{FF} = 1$, and the Si membrane thermal conductivity of 9 W/m/K (corresponding to thickness of 9 nm) were used in the calculations. The dotted lines shows the fundamental limit for thermal detectors when the detector and background temperature is 300 K.
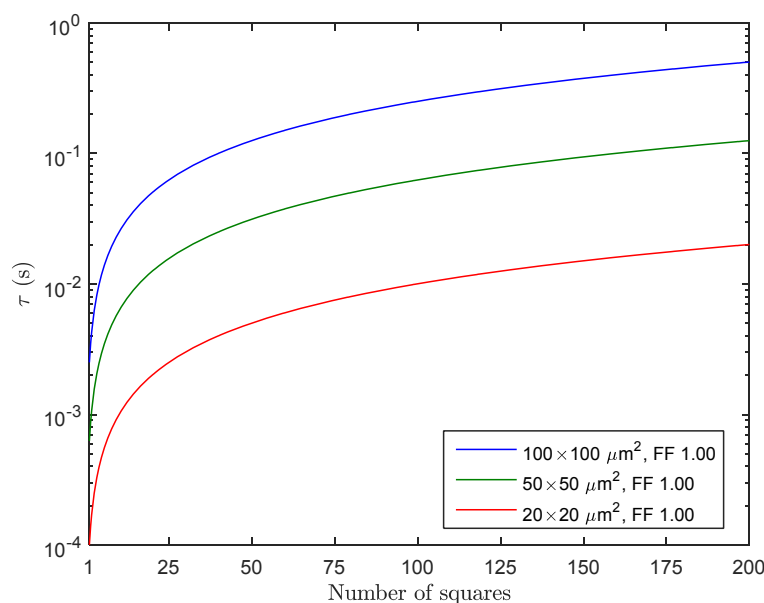
Figure 8. Calculated thermal time constant τ of the thermoelectric bolometers as functions of the number of squares in the thermocouple legs $N_{\square n} = N_{\square p}$. The indicated detector areas, the parameter values listed in Table 1, $\eta_{FF} = 1$, and the Si membrane thermal conductivity of 9 W/m/K (corresponding to thickness of 9 nm) were used in the calculations.

5. CONCLUSIONS

We have shown that thin silicon membranes can be used as high-performance active materials of thermoelectric bolometers. The estimated performance of these devices, both speed and sensitivity, increase remarkably when the thickness of the silicon membrane is reduced. Our calculations show that NEP below 1 pW/Hz$^{1/2}$ and time constant in the order of 1 ms can be achieved. Although silicon membranes with thickness of 6 nm [2] have been already fabricated, the fabrication of a complete bolometer with integrated optical absorber needs still to be demonstrated.

ACKNOWLEDGMENTS

REFERENCES

[1] Timofeev, A. V., Varpula, A., Shchepetov, A., Grigoras, K., Hassel, J., Ahopelto, J., Ylilammi, M. and Prunnila, M., "Thermoelectric bolometers based on ultra-thin heavily doped single-crystal silicon membranes," publishing in progress, manuscript available from arXiv:1704.02511.

[2] Shchepetov, A., Prunnila, M., Alzina, F., Schneider, L., Cuffe, J., Jiang, H., Kauppinen, E. I., Sotomayor Torres, C. M. and Ahopelto, J., "Ultra-thin free-standing single crystalline silicon membranes with strain control," Appl. Phys. Lett. 102, 192108 (2013).

[3] Neogi, S., Reparaz, J. S., Pereira, L. F. C., Graczykowski, B., Wagner, M. R., Sledzinska, M., Shchepetov, A., Prunnila, M., Ahopelto, J., Sotomayor-Torres, C. M., and Donadio, D., "Tuning Thermal Transport in Ultrathin Silicon Membranes by Surface Nanoscale Engineering," ACS Nano 9 (4), 3820 (2015).

[4] Chávez-Ángel, E., Reparaz, J. S., Gomis-Bresco, J., Wagner, M. R., Cuffe, J., Graczykowski, B., Shchepetov, A., Jiang, H., Prunnila, M., Ahopelto, J., Alzina, F. and Sotomayor-Torres, C. M, "Reduction of the thermal conductivity in free-standing silicon nano-membranes investigated by non-invasive Raman thermometry," APL Mater. 2, 012113 (2014).

[5] Dillner, U., Kessler, E. and Meyer, H.-G., "Figures of merit of thermoelectric and bolometric thermal radiation sensors," J. Sens. Sens. Syst. 2, 85 (2013).

[6] Richards, P. L., "Bolometers for infrared and millimetre waves," J. Appl. Phys 76 (1), 1 (1994).

[7] Talghader, J. J., Gawarikar, A. S. and Shea, R. P., "Spectral selectivity in infrared thermal detection," Light: Science & Applications 1, e24 (2012).

[8] Kruse, P. W., "A comparison of the limits to the performance of thermal and photon detector imaging arrays," Infrared Phys. Technol. 36, 869 (1995).

[9] Goldsmid, H. J., [Introduction to Thermoelectricity - Springer series in materials science 121], Springer, New York, 7-14 (2010).

[10] Stranz, A., Kähler, J., Waag., A. and Peiner, E., "Thermoelectric Properties of High-Doped Silicon from Room Temperature to 900 K," J. Electronic Materials 42 (7), 2381 (2013).